Applied Catalysis A: General 386 (2010) 51–59

Contents lists available at ScienceDirect

Applied Catalysis A: General

journal homepage: www.elsevier.com/locate/apcata

New oxidation catalysts based on iron(III) porphyrins immobilized on Mg–Al layered double hydroxides modified with triethanolamine

Kelly Aparecida Dias de Freitas Castro[a], Alesandro Bail[a], Pedro Braga Groszewicz[a], Guilherme Sippel Machado[a], Wido Herwig Schreiner[c], Fernando Wypych[b], Shirley Nakagaki[a,*]

[a] Laboratório de Química Bioinorgânica e Catálise, Universidade Federal do Paraná (UFPR), CP 19081, CEP 81531-990, Curitiba, Paraná, Brazil
[b] Laboratório de Química do Estado Sólido, Centro de Pesquisas em Química Aplicada - CEPESQ, Departamento de Química, Universidade Federal do Paraná (UFPR), CP 19081, CEP 81531-990, Curitiba, Paraná, Brazil
[c] Departamento de Física, Universidade Federal do Paraná (UFPR), CP 19081, CEP 81531-990, Curitiba, , Paraná, Brazil

ARTICLE INFO

Article history:
Received 19 April 2010
Received in revised form 14 July 2010
Accepted 18 July 2010
Available online 23 July 2010

Keywords:
Ironporphyrin
Oxidation
Catalysis
LDH
Triethanolamine
Immobilization
Heterogeneous catalysis

ABSTRACT

An Mg–Al layered double hydroxide containing intercalated NO_3^- anions (LDH-N) was synthesized and subsequently submitted to a reaction with triethanolamine as modifying agent (LDH-TEA). A neutral iron(III) porphyrin was immobilized onto both solids LDH-N and LDH-TEA, and the catalytic activity of the resulting FePor-LDH-N and FePor-LDH-TEA was evaluated in the oxidation of (Z)-cyclooctene, cyclohexane, and heptane using iodosylbenzene as oxidant. Characterization of FePor-LDH-N and FePor-LDH-TEA by UV–vis, FTIR, XRD, XPS, EPR, TGA/DTA, and SEM was also accomplished. The products from the catalytic reactions were analyzed by GC, using an FID detector. The catalytic activity of FePor-LDH-TEA in the oxidation of cyclohexane was around 5 times higher than that obtained with FePor-LDH-N, which does not contain the modifying agent. Moreover, the FePor-LDH-TEA solid displayed significant selectivity in the oxidation of heptane, a substrate that is difficult to oxidize; in fact, a total product yield over 30.0% was achieved. Finally, the performance of the FePor-LDH-TEA catalyst can be attributed to the higher FePor load in this solid, which is 3 times larger compared with FePor-LDH-N. A proposal concerning the mode of FePor immobilization onto the modified LDH is suggested.

1. Introduction

Metalloporphyrins are relevant examples of macrocyclic complexes that have attracted much attention over the last decades because of their role as efficient and selective catalysts in several oxidation reactions [1–6]. Despite their recognized catalytic activity toward the oxidation of hydrocarbons, the non-recyclability of these homogeneous catalysts has motivated researchers to seek for immobilization processes which could lead to heterogeneous catalysts with increased catalytic efficiency and higher selectivity [3,6–8]. Layered compounds are suitable materials for metalloporphyrin immobilization, including layered double hydroxides (LDH). The latter solids have recently been targeted because of their variable anionic exchange capacity and the possibility of chemically modifying their surface, which enable the controlled preparation of materials with specific composition for future potential industrial applications [9–14].

LDH consist of positively charged layers of metal hydroxide, stacked along the basal direction and separated by intercalated hydrated anions. The positive charges arise from the replacement of some divalent cations with trivalent ones, and the excess charge in the layers is balanced by intercalated anions. The LDH generic formula is $[M_{1-x}^{2+}M_x^{3+}(OH)_2]^{x+}(A^{n-})_{x/n}\cdot yH_2O$, where M^{3+} and M^{2+} are metallic cations occupying octahedron distorted sites and A is a hydrated anion with charge n^- [15,16].

LDH intercalation processes are widely discussed in the literature [9,15–21] and can be achieved through different methods, such as ion exchange, restructuring of layers of calcined samples through the memory effect, or direct synthesis in the presence of the anion to be intercalated. These methodologies may be monitored by X-ray diffraction (XRD), Fourier transformed infrared spectroscopy (FTIR), and thermal analyses (thermogravimetric analyses (TGA), differential scanning calorimetry (DSC), and/or differential thermal analyses (DTA)). XRD may also reveal the nature of the intercalated anions, according to the expansion of the basal spacing [17–23]. Intercalation of a series of metal complexes has been performed as a method for the production of mixed oxides [19,24] and complex/support catalysts [11,14,22,25–31].

In this work, along with the structural characterization of all the prepared materials, we have investigated the effects of the modification of an Mg–Al LDH with triethanolamine on the catalytic activity of an iron(III) porphyrin immobilized onto it.

* Corresponding author. Fax: +55 41 33613180.
E-mail address: shirley@quimica.ufpr.br (S. Nakagaki).

0926-860X/$ – see front matter © 2010 Elsevier B.V. All rights reserved.
doi:10.1016/j.apcata.2010.07.031

2. Experimental

2.1. Materials

The neutral iron(III)porphyrin [5,10,15,20-tetrakis(pentafluorophenyl)-1H, 23H-porphyrin iron (III) chloride] (FePor) was purchased from Sigma–Aldrich (St. Louis, United States). Iodosylbenzene (PhIO) was synthesized according to the literature by hydrolysis of iodosylbenzenediacetate [32]. The resulting solid was carefully dried under reduced pressure and kept at 5 °C, and its purity was periodically controlled by iodometric titration [33]. Deionized water was employed in all the experimental procedures. Unless otherwise specified, all other reagents were supplied by Sigma–Aldrich or Acros (Geel, Belgium) and used as received without further purification.

Mg–Al LDH intercalated with nitrate anions was prepared as described previously [34]. Under inert atmosphere, a sodium hydroxide solution was added to a solution of magnesium and aluminum nitrate salts previously prepared at the appropriate stoichiometry, and the pH was controlled to 10. The resulting white solid (LDH-N) was exhaustively washed with water, centrifuged at 4000 rpm, and dried at 50 °C for 48 h.

In a reaction flask, 15 mL triethanolamine (TEA) were added to 0.5217 g LDH-N, and the system was kept under reflux conditions and stirring for 3 h. The obtained brown viscous suspension was centrifuged, and a light brown solid (LDH-TEA) was separated and then washed several times with isopropanol, followed by drying at 60 °C [35].

The FePor-LDH-X (where X = N or TEA) catalysts were prepared according to a methodology described in the literature [22]. The immobilization process was conducted by dispersing around 150 mg of the support (LDH-N or LDH-TEA) in 10 mL of a toluene FePor solution (4.69×10^{-6} mol FePor). This suspension was refluxed and stirred for 2 h. Next, the resulting solid was filtered and washed with toluene, and the supernatant was analyzed by UV–vis spectroscopy, in order to quantify the FePor that could have been removed from the matrix by leaching. The light brown solids FePor-LDH-X were dried at 60 °C for 48 h.

2.2. Catalytic oxidation reactions

Catalytic oxidation reactions were carried out in a 2 mL thermostatic glass reactor equipped with a magnetic stirrer, placed inside a dark chamber. The oxidation of (Z)-cyclooctene (previously purified on alumina column), cyclohexane, and heptane by iodosylbenzene was accomplished in the presence of the catalyst FePor-LDH-N or FePor-LDH-TEA. In a standard experiment, the solid catalyst FePor-LDH-X and the oxidant (FePor/PhIO molar ratio 1:50) were suspended in 400 μL solvent (dichloromethane/acetonitrile 1:1 mixture, v/v) and degassed with argon for 15 min, inside a 2 mL vial. The reaction started after addition of the substrate (FePor/substrate molar ratio 1:5000), and the oxidation reaction was carried out under magnetic stirring for 1 h. At the end of the reaction, sodium sulfite was added to the reaction mixture, in order to eliminate the excess iodosylbenzene. The supernatant along with the reaction products were separated from the solid catalyst by centrifugation and transferred to a volumetric flask. The catalyst was washed several times with dichloromethane and acetonitrile, in order to extract any reaction products that might have remained adsorbed onto the solid catalyst. The washing solutions were added to the previously separated reaction supernatant, and the product content in these combined solutions was analyzed by gas chromatography, using *n*-octanol (acetonitrile solution, 1.0×10^{-2} mol L^{-1}) of high purity degree (99.9%) as internal standard. Product yields were based on the mass of PhIO added to each reaction.

The influence of reaction time on product yield and selectivity was investigated for the solid with the best catalytic performance, with reaction times ranging from 15 min to 72 h. Control reactions were carried out using this same procedure, and were performed as follows: (a) substrate only, (b) substrate + PhIO, and (c) substrate + PhIO + LDH-X (supports without FePor). A solution of the parent FePor also had its catalytic activity (homogeneous catalysis) measured in the same conditions as those employed for the solid catalysts FePor-LDH-X. All heterogeneous catalysts were exhaustively washed and dried for reuse in further reactions.

2.3. Characterization techniques

Electronic spectra (UV–vis) were obtained on an HP 8452A Diode Array UV–vis spectrophotometer, in the 200–800 nm range. Spectra of the solid samples were recorded from nujol mull smeared on a quartz plate (Hellma).

Transmission Fourier Transform Infrared (FTIR) spectra were registered on a Biorad 3500 GX spectrophotometer in the 400–4000 cm^{-1} range, using KBr pellets. KBr was ground with a small amount of the solid to be analyzed, and the spectra were collected with a resolution of 4 cm^{-1} and accumulation of 32 scans.

For the X-ray diffraction (XRD) measurements, self-oriented films were placed on neutral glass sample holders. The measurements were performed in the reflection mode using a Shimadzu XRD-6000 diffractometer operating at 40 kV and 40 mA (Cu Kα radiation λ = 1.5418 Å) with a dwell time of 1°/min.

Electron paramagnetic resonance (EPR) measurements of the powder materials were accomplished on an EPR BRUKER ESP 300E spectrometer (standard concavity: 4102-SP, frequency X band 9.5 GHz), at room temperature or at 77 K (using liquid N_2).

X-ray Photoelectron Spectroscopy (XPS) spectra were measured on a VG ESCA 3000 with a base pressure of 2×10^{-10} mbar. Mg Kα (1253.6 eV) radiation was employed, and the overall energy resolution of the collected spectra was approximately 0.8 eV. The energy scale was calibrated using the Fermi level and the adventitious C 1s peak at 284 eV. The spectra were normalized to the maximum intensity after subtraction of a constant background.

Scanning Electron Microscopy (SEM) characteristics of the samples were imaged by either a JEOL 5190 microscope operating at 15 keV or a JEOL JSM-6360LV operating at 15 keV. A small amount of the sample was placed on a sample holder, which was submitted to a gold metallization process and measured by a scan mode. The cross-section analyses were performed by electron dispersive X-ray (EDX). Mapping of elements was carried out to investigate the distribution of these elements in the surface layers. The Image Pro Plus software was employed to process the images

Products from catalytic oxidation reactions were quantified using a Shimadzu GC-14B gas chromatograph (FID detector) equipped with a DB-WAX capillary column (J & W Scientific).

3. Results and discussion

A dark yellow solid was obtained after reaction between TEA and LDH-N, suggesting that the modification was successful. Both solids LDH-TEA and LDH-N were characterized by XRD, EDX, XPS, TGA/DTA, FTIR, and SEM.

Although the XRD patterns revealed broad peaks, the first basal diffraction peak of LDH-N (Fig. 1b) shifted from 8.10 Å to only 8.45 Å in LDH-TEA (Fig. 1a). Since the peak shift was not large, one might believe the intercalation reaction was not successful.

Previous studies on the intercalation and functionalization of layered materials by TEA found that the thickness of a single layer of this molecule between inorganic layers is around 4 Å [35]. Consequently, the intercalation of TEA in LDH-N should not change the

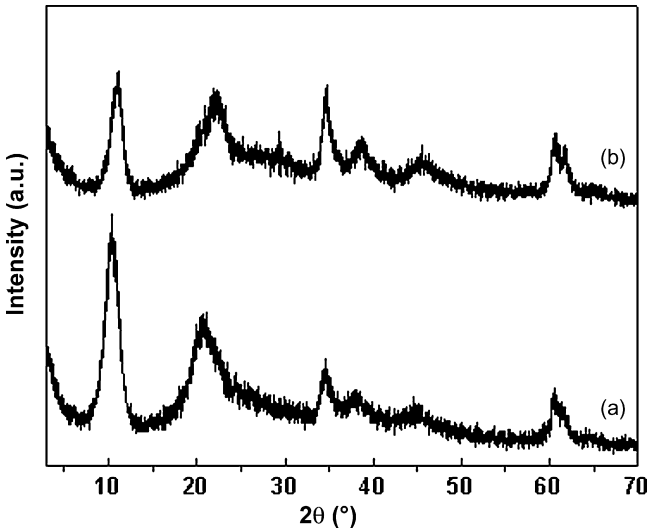

Fig. 1. X-ray powder diffraction patterns for (a) LDH-TEA and (b) LDH-N.

basal distance much, for 4 Å is roughly the same space occupied by nitrate anions in LDH-N. Therefore, the use of other techniques was necessary to confirm the presence of TEA intercalated between the LDH layers.

EDX analyses (data not shown) attested the presence of Mg, Al, O, N, and C in LDH-N. While the first four elements were expected, the presence of carbon can be assigned to contamination of LDH-N by a small content of carbonate anions in the LDH, since this anion is commonly found in this class of compounds [36]. Moreover, from this analyses it was established that the Mg/Al ratio is around 3:1. The same elements Mg, Al, O, N, and C were detected in the LDH-TEA EDX analyses, which also confirmed the 3:1 ratio between Mg and Al. This means that the LDH layer composition remained the same after reaction with TEA. Moreover, higher percentages of C and N were observed, which could be evidence of the presence of TEA. XPS analyses confirmed this information. In a wide scan of both LDH-TEA and LDH-N (Fig. 2a and b), electrons from Mg_{2p}, Al_{2p}, and O_{1s} were detected with binding energies of 50.6, 75.0, and 531.5 and

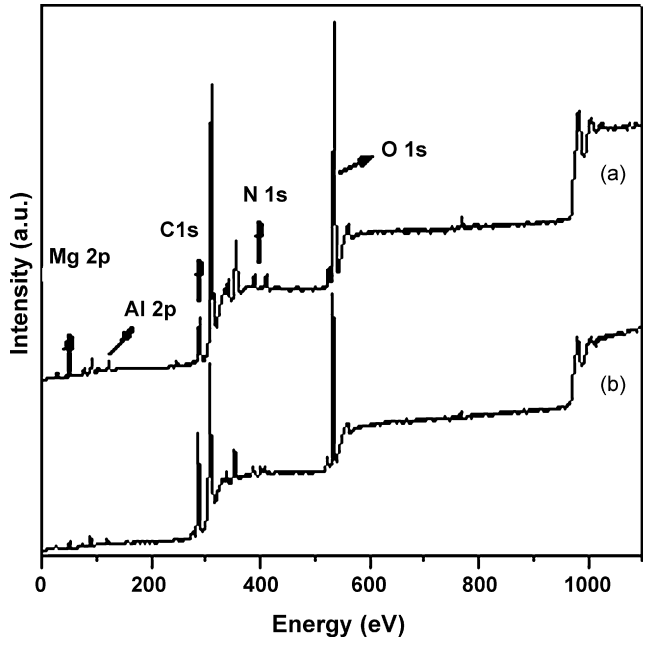

Fig. 2. Low-resolution XPS spectra of (a) LDH-TEA and (b) LDH-N.

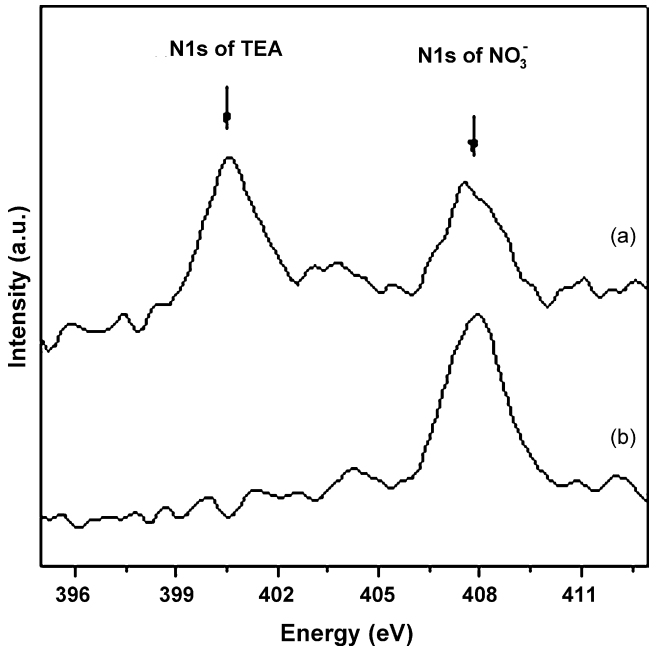

Fig. 3. High-resolution XPS spectra of (a) LDH-TEA and (b) LDH-N.

532.3 eV, respectively [37]. Peaks in the region of N_{1s} and C_{1s} were also observed; the latter, which is related to adventitious carbon, was used to calibrate the spectra.

The ratio between areas of two peaks of elements enables determination of their relative abundance on a surface. The N/Al ratio in the LDH rose from 0.77 to 1.11 upon LDH-N modification with TEA, which is evidence of increased nitrogen content. This relative elevation in nitrogen content is thus another evidence of the presence of TEA in the LDH, since TEA was the only source of nitrogen during the modification reaction.

In order to further characterize this nitrogen excess, higher resolution spectra of the N_{1s} region were recorded for both materials (Fig. 3). While the spectrum of LDH-N displayed only one peak, corresponding to nitrate N_{1s}, the spectrum of LDH-TEA presented two peaks, the first (from right to left) related to nitrate and the other to TEA. Comparison of both spectra led to attribution of the 408 eV peak to nitrate due to its binding energy [38]. A lower binding energy should be expected for TEA N_{1s}, since the electronic shielding of the nucleus charge by valence electrons is more effective in the latter molecule than in the nitrate anion, where the valence electrons are attracted away from the nucleus by the oxygen atoms.

Thermal analyses curves of these materials gave further evidence of the presence of TEA in the modified LDH. According to Fig. 4b, there are two mass loss events for LDH-N, around 200 °C and 450 °C. The first event can be attributed to evaporation of intercalated/physisorbed water molecules (mass loss = 15%), while the second is characteristic of dehydroxilation reaction and decomposition of intercalated nitrate (mass loss = 36%). All these events are endothermic, as shown by DTA, and their temperatures match those reported for nitrate-intercalated Mg–Al LDH [39], showing that carbonate contaminations are very small. Also, the mass loss percentages of these events match those calculated for a 3:1 Mg/Al ratio.

Although LDH-TEA also undergoes two mass loss events, its TGA curve (Fig. 4a) differs from that of LDH-N with respect to its larger total mass loss. While the second event remains unchanged (mass loss = 35%), the first one amounts to a mass loss of 23%, which accounts for the difference in total mass loss. This increased mass loss up to 200 °C for LDH-TEA can be assigned to evaporation of

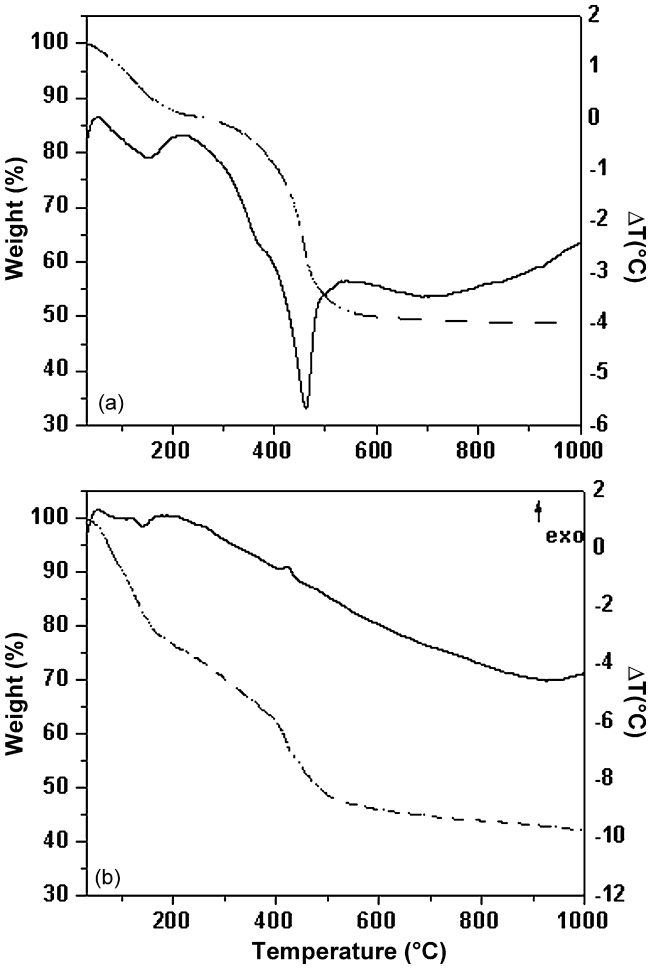

Fig. 4. Thermal analyses (TGA/DTA) curves of (a) LDH-TEA and (b) LDH-N.

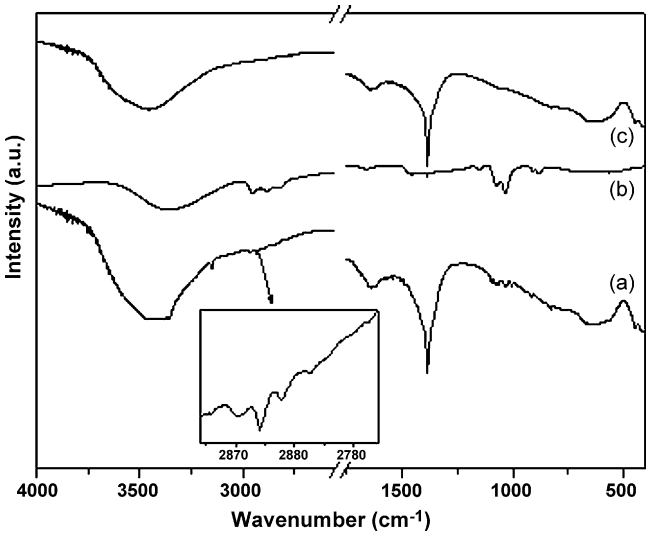

Fig. 5. FTIR spectra of (a) LDH-TEA, (b) TEA, and (c) LDH-N.

intercalated TEA, which is probably held to the layers solely by weak interactions. Conversely, a small exothermic event centered at 460 °C followed by a steeper mass loss, which are both characteristic of combustion of organic matter, might suggest grafting of some TEA molecules onto the LDH layers. These grafted TEA would be covalently bound to the LDH, and would therefore burn instead of evaporate [35].

In order to shed light on the nature of the interaction between TEA and LDH layers, FTIR spectroscopy was performed on these materials. Along with the above mentioned techniques, the FTIR analyses revealed that only a small amount of the modifier is present in the LDH after interaction with TEA. The infrared spectra showed differences between the LDH-N and the solid obtained after reaction with TEA (Fig. 5). In the latter case, there was an absorption band in the region of 3600–3200 cm^{-1}, centered at 3464 cm^{-1}, which can be ascribed to the OH group present on the surface of the LDH as well as to the hydroxyl groups present in TEA ($C_6H_{15}O_3N$). The absorption band at 1385 cm^{-1} is due to the nitrate ion and indicates that these ions are present in the interlayer space of LDH-TEA. This band thus suggests that not all the nitrate ions were exchanged [40] as already evidenced by XPS analyses (Figs. 2 and 3).

Moreover, bands characteristic of the vibration modes of symmetric and asymmetric CH groups present in TEA were detected in the region of 2900–2850 cm^{-1}, as well as bands in the region of 1260–1350 cm^{-1}, typical of the C–O chemical bond observed after intercalation with TEA [41].

Evidence that some of the TEA molecules may be grafted onto the LDH layers is the presence of a characteristic absorption band of bound hydroxyl groups [41] centered at 3150 cm^{-1}. In this sense, it is expected that the grafting should occur between the highly hydroxylated surface of the LDH and the modifying agent and also be attached through a hydrogen bond between the LDH layer and the OH group on the surface of the modifier.

Thus, the different hydroxyl groups evidenced by the FTIR spectra suggest the presence of a small amount of grafted TEA, whereas the remaining TEA molecules are intercalated. Some characteristic bands of TEA, such as the C–N stretching bands in the region of 1310–1360 cm^{-1}, could not be seen in the FTIR spectrum due to the low concentration of the modifier in the LDH and the very intense bands characteristic of the nitrate anion. Also, other bands typical of CH_2 groups were hard to detect. The absorption bands observed in the regions of lower frequency, namely in the region of 850–400 cm^{-1}, can be assigned to M–O and O–M–O (M = metal) vibrational modes [41].

When inorganic ions predominantly intercalate into the LDH, SEM images usually have platy morphology with hexagonal habits, bound in such a way that many authors call them “pink sand” (Fig. 6b) [42]. In contrast, when organic anions intercalate into the LDH, the formation of round-edged particles is observed [42]. LDH-TEA does not present hexagonal crystals, as expected, since it was modified with organic molecules and submitted to the stirring process. Fig. 6a shows that the particles tend to agglomerate, and it significantly differs from the image obtained for LDH-N, containing intercalated nitrate anions (Fig. 6b).

As for FePor immobilization onto the LDH-X, modification of the support caused higher percentage of complex immobilization and hence higher FePor concentration on the matrix. Table 1 lists the FePor loading in the FePor-LDH-X catalysts, which was determined by UV–vis spectroscopy, as described in the experimental section

The way this neutral FePor is immobilized onto the LDH support is not completely understood. Interactions between the π-conjugated cloud of the macrocyclic ring of the FePor and the highly hydroxylated surface of the LDH cannot be dismissed, together with some kind of interaction between the modifying agent of the coverslip and the FePor. In addition to these two possibilities, the suggestion that the FePor might also be caught between the random “house-of-card” structure probably acquired by the LDH layers during the magnetic stirring process cannot be overlooked. All these proposals are still under investigation.

Fig. 7 depicts some of the proposed modes of FePor immobilization onto the surface of the LDH-N and LDH-TEA supports.

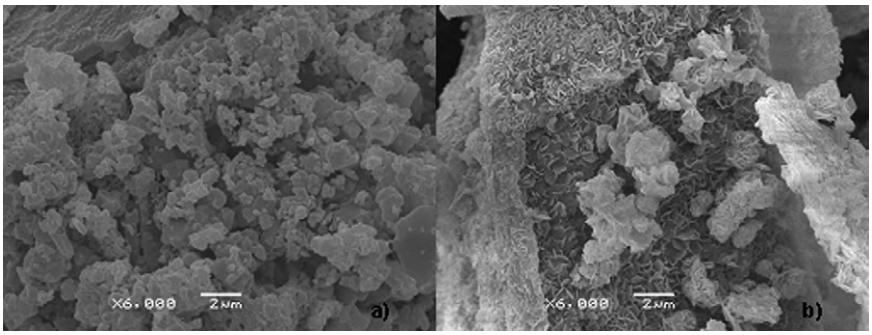

Fig. 6. SEM micrographs of (a) LDH-TEA and (b) LDH-N.

Table 1
Immobilization of FePor on LDH.

	FePor immobilization (%)	Loading (concentration of FePor in the LDH) (mol g^{-1})
FePor-LDH-N	17.4	3.2×10^{-6}
FePor-LDH-TEA	54.0	1.0×10^{-5}

Fig. 7a brings two proposals representing the interaction between the metallic center of the macrocycle and the highly hydroxylated surface of the support. These representations differ only in terms of the positioning of the porphyrin: tilted (top) and parallel to the layer (bottom).

According to the TGA results, the Mg/TEA molar ratio is approximately 1:7. On the basis of the large amount of modifying agent in FePor-LDH-TEA, in Fig. 7b it is suggested that TEA may be present in two positions, on the surface of and intercalated between the LDH layers. In this sense, it can be assumed that FePor immobilization might take place via interaction between the π-conjugated electronic cloud of the meso porphyrin-substituents and the modifying agent.The XRD pattern of FePor-LDH-N (Fig. 8b) is similar to that obtained for the LDH-N support, indicating that immobilization does not occur by FePor intercalation in the LDH [20]. However, a diffraction peak at 7.10° of 2θ (peak indicated by an arrow), related to a basal distance of 12.45 Å, is observed for FePor-LDH-TEA (Fig. 8a). The presence of this peak suggests that part of the FePor may also intercalate between the layers of the support previously modified with TEA.

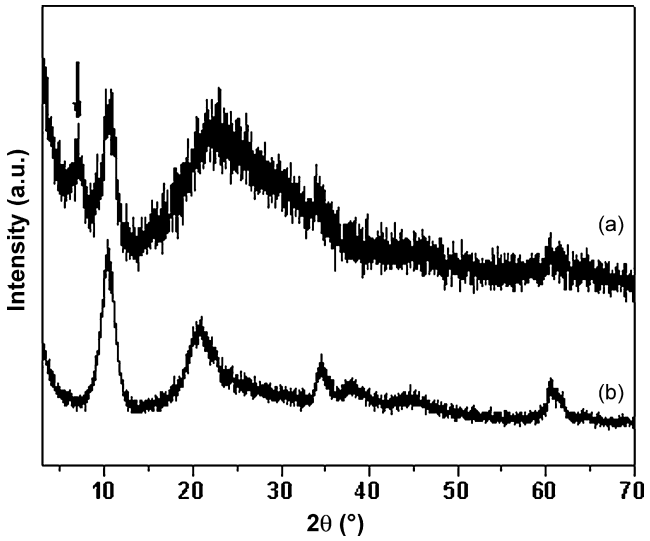

Fig. 8. X-ray powder diffraction patterns for (a) FePor-LDH-TEA and (b) FePor-LDH-N.

Compared with the spectrum of LDH-TEA (Fig. 2), changes in the XPS spectrum of FePor-LDH-TEA (Fig. 9) confirmed the presence of the FePor in the latter solid, which was evident from the higher concentration of carbon and the increased N/Al ratio. However, it

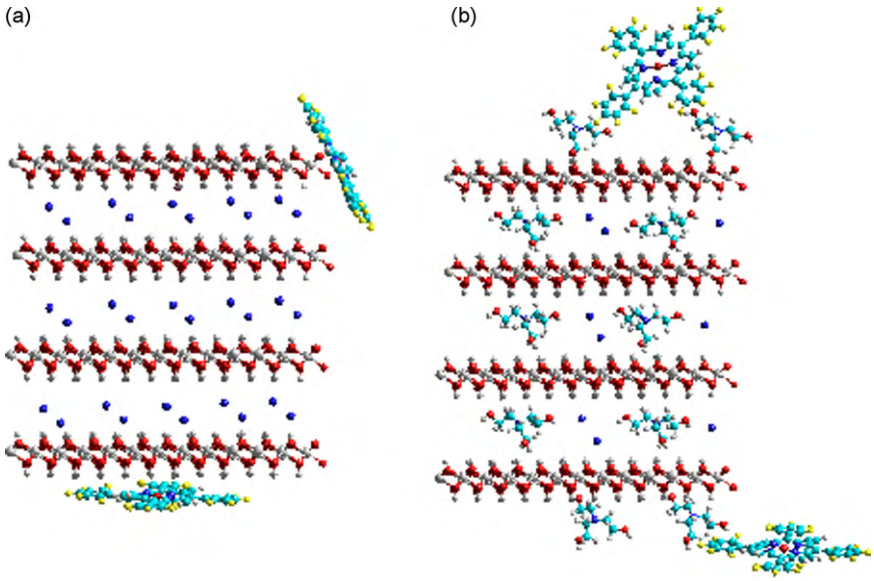

Fig. 7. Proposed modes of FePor immobilization onto the LDH support. (a) FePor-LDH-N interaction between the FePor metallic center and the hydroxilated surface of the support, and (b) FePor-LDH-TEA immobilization by interaction between the meso substituent on the FePor and the modifying agent.

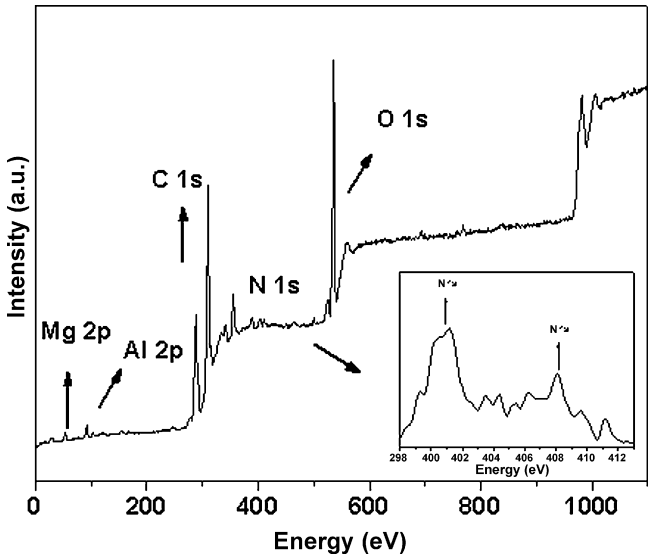

Fig. 9. Low-resolution XPS spectra of (a) FePor-LDH-TEA.

was not possible to detect the presence of iron, which was below the detection limit of the technique.

The presence of FePor in the FePor-LDH-X solids was also confirmed by EPR spectroscopy. The LDH-X solids (figure not shown) display EPR-silent spectra. The absence of EPR signals indicates that the solids are free of contaminating paramagnetic species that could have been inserted into the LDH during the synthetic procedure.

Both FePor-LDH-TEA and FePor-LDH-N (Fig. 10b and c, respectively) display an EPR signal at $g = 4.3$, typical of high-spin Fe(III) in rhombic symmetry, while a signal at $g = 6.0$ (1000–1200 gauss) is observed in the spectrum of the free FePor (Fig. 10a), which is characteristic of high-spin Fe(III) in axial symmetry [43]. These results demonstrate that the immobilization procedure causes an orthorhombic distortion in almost all porphyrin rings [44]. This distortion can be associated with the need of the porphyrin to remain as close as possible to the hydroxylated surface, in order to maximize charge interactions, which might reinforce the model presented in Fig. 7 [44].

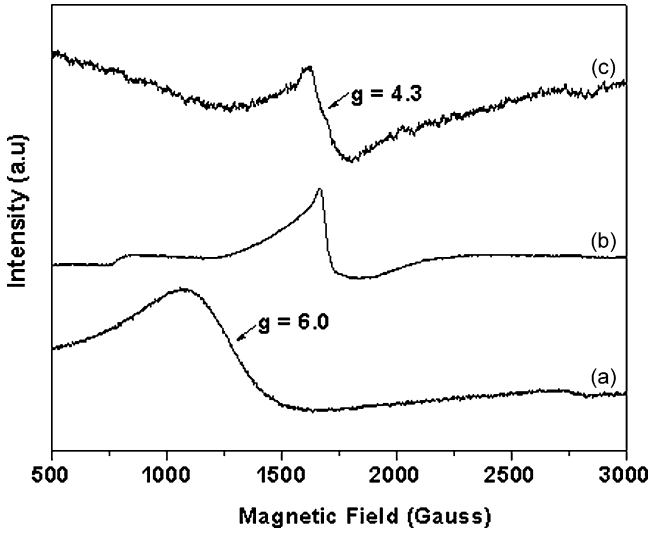

Fig. 10. Room temperature EPR spectra of (a) FePor, (b) FePor-LDH-TEA, and (c) FePor-LDH-N.

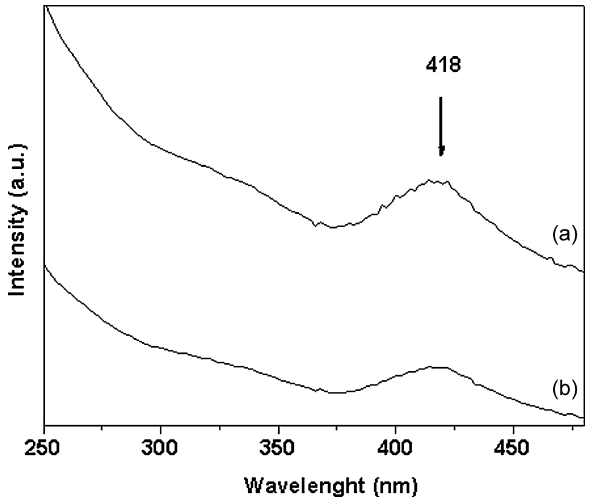

Fig. 11. UV–vis spectra of (a) FePor-LDH-TEA and (b) FePor-LDH-N.

Table 2
(Z)-cyclooctene oxidation by PhIO catalyzed by FePor in homogeneous and heterogeneous media[a].

Catalyst[b]	Run	Epoxide (%)
FePor	1	76.0
FePor-LDH-N	2	66.0
FePor-LDH-TEA	3	97.8
LDH-N + PhIO (control)	4	10.5
LDH-TEA + PhIO (control)	5	10.2
PhIO (control)	6	5.0

[a] The yield of cyclooctene oxide was calculated on the basis of the amount of PhIO used in the reaction. The results represent an average of at least duplicate reactions. FePor/PhIO/(Z)-cyclooctene molar ratio = 1:50:5000. Reaction time: 1 h.

The FTIR spectra of all the FePor-LDH-X solids were similar to those of the corresponding LDH-X matrix prior to FePor immobilization (figure not shown). Vibrational bands of the FePor were not detected in the FTIR spectra probably because of the low FePor loading on the solids (Table 1).

The FePor-LDH-X solids were also analyzed by UV–vis spectroscopy (Fig. 11). The presence of FePor was confirmed by the typical FePor Soret band that appeared in the region of 400 nm in both spectra. Also, the recorded spectra displayed a typical peak enlargement observed for metalloporphyrin bound to solid supports [45].

However, in the spectra of Fig. 11 the Soret band is shifted to lower energy compared to the spectrum of the parent FePor registered before the immobilization process (spectrum collected in Nujol oil emulsion – figure not show). Such shift can result from the confinement of the FePor in the support or from interactions between the FePor and the surface of the support, both of which may distort the structure of the FePor complex [46].

4. Catalytic oxidation reactions

The catalytic activities of the FePor in solution (homogeneous catalysis) and of the supported catalysts FePor-LDH-X (heterogeneous catalysis) were investigated in the oxidation of (Z)-cyclooctene, cyclohexane, and heptane. The results are displayed in Tables 2–4, respectively.

The catalytic yields depicted for FePor-LDH-N and FePor-LDH-TEA in these tables can be attributed to the immobilized FePor, since control reactions carried out with the pure matrices LDH-N and LDH-TEA (containing no FePor) gave only low yields of products.

Table 3
Cyclohexane oxidation by PhIO catalyzed by FePors in homogeneous and heterogeneous media[a].

Catalyst	Run	Alcohol yield (%)[b]	Ketone yield (%)[c]
FePor	1	51.0	2.0
FePor-LDH-N	2	7.5	3.6
FePor-LDH-TEA	3	26.4	2.2
FePor-LDH-TEA Recycling run 1	4	23.0	2.0
FePor-LDH-TEA Recycling run 2	5	25.8	1.0
FePor-LDH-TEA Recycling run 3	6	25.7	1.2
LDH-N + PhIO (control)	7	Trace	0
LDH-TEA + PhIO (control)	8	Trace	0
PhIO (control)	9	Trace	–

[a] The yields of the reactions were calculated on the basis of the amount of PhIO used in the reaction. The results represent an average of at least duplicate reactions. FePor/PhIO/cyclohexane molar ratio = 1:50:5000. Reaction time: 1 h.
[b] Cyclohexanol
[c] Cyclohexanone.

5. Cyclooctene

Cyclooctene is easily oxidized in the presence of metalloporphyrins, leading to a single product, an epoxide. This is consequence of the larger stability of the radical intermediate generated from this substrate and which furnishes the epoxide [47,48]. For this reason, cyclooctene is frequently employed as a diagnostic substrate in catalytic systems involving metalloporphyrins. The catalytic oxidation of this cycloalkene by PhIO was of great value for this work, because it demonstrated the efficiency and stability of the immobilized FePor-LDH-X as catalysts. This study also provided information on the accessibility of the substrate and the oxidant to the iron(III) sites of the intercalated FePor.

The results from the epoxidation of cyclooctene by PhIO catalyzed by FePor in solution or by FePor-LDH-X are summarized in runs 1–3 of Table 2.

As expected, high epoxidation yields were observed for the FePor in solution. The enhanced catalytic activity of this complex with respect to oxidation reactions is due to the presence of electronegative substituents on its phenyl rings, which reduce electronic density on the porphyrin ring and stabilize the FePor against oxidative degradation [49].

All the FePor-LDH-X solids displayed catalytic activity for (Z)-cyclooctene oxidation, thus confirming that the immobilization process and the experimental conditions did not destroy or inactivate the immobilized FePor (Table 2). However, the yield was slightly lower in the case of FePor-LDH-N, which can be associated with the difficult access of the substrate and the oxidant to the active site of the FePor, limited by the structure of the support [26].

Compared with homogeneous catalysis (run 1), a higher product yield was observed when FePor-LDH-TEA was employed as catalyst (run 3). Hence, immobilization favored the catalytic activity of the FePor in this case.

Comparison of the results obtained for the homogeneous system (FePor in solution) and the FePor-LDH-X systems shows that the FePor does not undergo any deactivation processes, such as hindered access of the reagents to the catalytic site or iron(III) axial coordination to ligands on the support.

Control reactions (reactions 4–5) were also accomplished, and very low yields were observed. Comparison of these results with those achieved in the reactions catalyzed by the FePor-LDH-X solids confirms that the immobilized FePor plays an essential role in the investigated reactions.

A UV–vis spectrum of the reaction supernatant was recorded after the catalytic reactions in the presence of FePor-LDH-X. The typical Soret band of the FePor was not detected in any of the cases, attesting that no catalyst leaching occurred under any of the reaction conditions investigated in this study, and that the catalysis was truly heterogeneous.

6. Cyclohexane

As both immobilized catalysts FePor-LDH-X were efficient for the epoxidation of cyclooctene (showing yields higher than 50%), their catalytic activity was also evaluated in the oxidation of cyclohexane (Table 3), a less reactive substrate. The use of cyclohexane as substrate is intended not only for evaluation of the catalytic efficiency toward the oxidation of a different compound, but also for the investigation of the catalyst's effect on reaction selectivity, since more than one product might be produced in the oxidation of this cycloalkane.

The oxidation of cyclohexane by PhIO in the presence of metalloporphyrins commonly yields cyclohexanol and cyclohexanone as major products, so these catalysts are considered cytochrome P-450 biomimetic models [49,3]. High selectivity for the alcohol product is also observed. Alcohol formation occurs via oxygen transfer from the intermediate oxoiron(IV) porphyrin cation radical complex, which is the active species responsible for the hydroxylation reaction [5,49–51].

The formation of the latter intermediate occurs upon oxidation of the FePor by a two-electron oxidant such as PhIO [41]. The formed species, which is supposed to be catalytically active, will abstract one proton from the substrate, generating a radical from it. In turn, this radical species will react with the hydroxyl coordinated to the iron complex and reestablish the FePor [5,3,50–53], with concomitant formation of an alcohol, which can be re-oxidized to the ketone.

Good yields were obtained with the FePor-LDH-X supported catalysts (Table 3, runs 2 and 3). However, these results might be considered low if compared to those achieved via homogeneous catalysis (Table 3, run 1). When the different matrices were compared, better results were obtained with the FePor-LDH-TEA system, which presents a less polar support, due to the partial coverage of the highly hydroxylated surface of the LDH support with TEA molecules (Fig. 7). As the substrate cyclohexane is only slightly polar, its access is favored [50] in the latter system, and the product cyclohexanol (more polar) is also more rapidly released from the active site into the solution, preventing its further oxidation to the ketone. In fact, the more polar system FePor-LDH-N leads to lower cyclohexanol yields and lower selectivity for the alcohol, compared with FePor-LDH-TEA.

So, although the catalyst FePor-LDH-TEA furnished lower alcohol yields compared to the homogeneous catalyst (27% and 51% cyclohexanol yield, respectively), it is still highly selective, as expected for cytochrome P-450 models, not to mention the major advantage that this solid catalyst is recyclable. Table 3 (runs 4–6) also lists the results achieved in reactions employing FePor-LDH-TEA after it was recovered from the reaction medium and reused. Reuse of this solid (recycling) had little if no effect on its catalytic efficiency and selectivity.

Catalyst reuse in a second reaction led to yields similar to those obtained with the fresh catalyst in a first reaction, suggesting that FePor-LDH-X can be reused. The catalytic activity in the recycling reactions also indicates resistance of the FePor to the harsh reaction conditions and gives evidence of the strong interaction between the FePor and the support. FePor-LDH-X was recovered after the first use by simple filtration and washing in a Soxhlet extractor. In fact, all reaction solutions analyzed after the catalytic reactions and recovery procedure failed to display the characteristic FePor Soret. After the second use, the catalyst was recovered and reused in a third reaction, giving similar results, which was also observed in three more subsequent reactions.

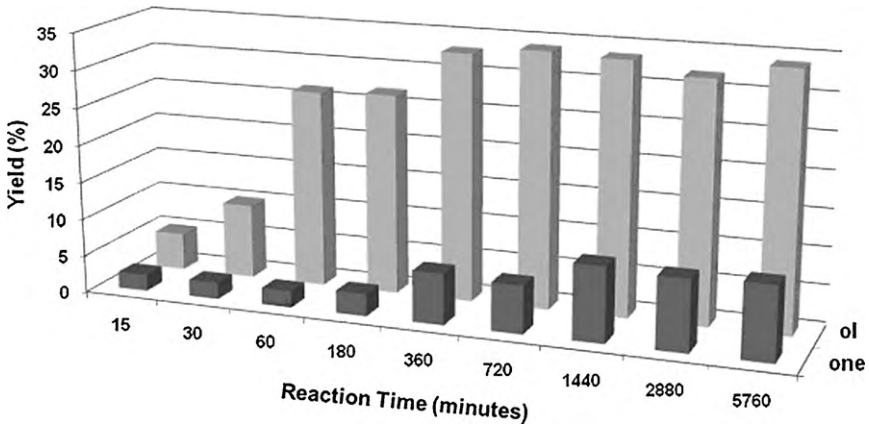

Fig. 12. Catalytic reactions on cyclohexane oxidation. Yield based in cyclohexanol and cyclohexanone.

The solid that exhibited the best performance toward the catalytic oxidation of cyclohexane by PhIO, together with small loss of catalytic efficiency after recycling processes was FePor-LDH-TEA (Table 3, reaction 3). Hence, this solid was used in a study about the influence of reaction time on product yields.

In general, better yields are not expected with increasing reaction times for this FePor in homogeneous medium, since the optimal reaction time reported in the literature was employed here [6,12,22,31]. As for heterogeneous catalysis, an increase in reaction time is expected to lead to better yields, as shown in Fig. 12. This can be explained by longer contact time between the solid catalyst and the substrate, thereby facilitating access of the latter to the immobilized active catalytic species and favoring the catalysis.

Fig. 12 reveals that the optimal reaction time is about 1 h, when selectivity and good catalytic efficiency are achieved. An increase in time might lead to better yields; however, the reaction becomes less selective. After 6 h of reaction, the equilibrium with respect to the formation of cyclohexanol is reached (34%). After this time, it is observed that the generated alcohol is re-oxidized to cyclohexanone.

Although the yields measured in this study were lower than those reported in the literature (for example, the system MgAl-3APTS LDH-FePor yielded 36% alcohol and 57% ketone, with a selectivity of 1.6 for the ketone [22], with the same FePor), the FePor-LDH-TEA catalyst described here is more selective (26.4% alcohol and 2.2% ketone, giving a selectivity of 12 for the alcohol).

In order to know some rate information about the cyclohexane oxidation the first-order kinetics was qualitatively applied for the cyclohexane oxidation reaction results using the FePor-LDH-TEA as catalysts, according to the equation: $\ln[P]_\infty/[P]_\infty - [P]_t = k{\cdot}t$, where $[P]_\infty$ is the product molar concentration (cyclohexanol + cyclohexanone) at infinite time (6 h), $[P]_t$ is the product molar concentration at time (t) and k is the first-order reaction constant (min^{-1}). In this treatment the amount of catalyst was considered constant. It is well known that the rate constant (k), is determined from the slope of the linear first-order kinetic graphic. The k obtained in this qualitative treatment was 9.97×10^{-3} min^{-1} (1.5835×10^{-4} s^{-1}), similar to the values observed for other heterogeneous oxidation catalyst [54]. The rate constants of the oxidation products formation using metalloporphyrins as catalyst in homogeneous catalysis is about 4.0×10^{-4} s^{-1} [55]. The lower value for the rate constant qualitatively obtained in the present work was expected since in the heterogeneous catalysis, the diffusion of the oxidant and substrate to and from the immobilized catalytic site should be considerably slow [56].

Since FePor-LDH-TEA was the best catalyst in the oxidation of cyclohexane, it was also tested in the oxidation of heptane, which is a linear alkane and, therefore, is more resistant to oxidation. The oxidation of heptane can lead to the formation of different alcohols and ketones, and the regioselectivity of the reaction (oxidation at positions 1, 2, 3, or 4 of the carbon chain) depends on the structure of the employed catalyst [57,58].

Many catalytic systems based on metalloporphyrins have been developed for oxidation of linear alkanes in recent years; however, few systems were selective for the terminal positions. Despite the difficulty in obtaining efficient and selective catalysts for this type of oxidation, the research is intense because the oxidation products, such as alcohols and ketones, are widely employed in the industry, so the oxidation of terminal positions is a major challenge for researchers [59].

Table 4 presents the results from the oxidation of heptane by PhIO catalyzed by FePor in homogeneus and heterogeneous media. In both cases, selectivity for the alcohols is observed.

FePor-LDH-TEA (run 2) was more selective and efficient than the parent FePor in homogeneous solution (run 1). The majority of products consisted of alcohols generated from oxidation at posi-

Table 4
Heptane oxidation by PhIO catalyzed by FePor in homogeneous and heterogeneous media[a].

Catalyst	Run	Heptane/(%)									
		1-ol	2-ol	3-ol	4-ol	[b]Total ol	2-one	3-one	4-one	[c]Total one	ol/one
FePor	1	1.7	15.0	15.2	1.7	33.6	<1	1	<1	2.0	16.8
FePor-LDH-TEA	2	3.5	10.2	10.6	5.0	29.3	–	3.5	–	3.5	8.4
Recycling run	3	3.0	10.0	9.0	4.0	26.0	–	2.0	–	3.0	8.6
LDH-TEA + PhIO(control)	4	–	–	–	–	–	–	–	–	–	–
PhIO (control)	5	–	–	–	–	–	–	–	–	–	–

[a] The yields of the reactions were calculated on the basis of the amount of PhIO used in the reaction. The results represent an average of at least duplicate reactions. FePor/PhIO/heptane molar ratio = 1:50:5000. Reaction time: 1 h.
[b] Heptanol
[c] heptanone.

tions 2 and 3 of heptane, which are more readily oxidized due to the higher stability of the organic radical formed on secondary carbon atoms. However, some oxidation at position 1 was also observed, in higher percentage compared the homogeneous reaction.

Reactions with metalloporphyrins in homogeneous systems are usually selective for the alcohol and regioselective at positions 2 or 3, because less energy is necessary for the oxidation taking place at these positions compared with position 1 [58]. Apparently, only Suslick and co-authors [58] observed some selectivity for position 1 of hexane when they used metalloporphyrin-based systems.

Also, it was observed that the FePor-LDH-TEA solid still displayed catalytic activity when it was further reused, with results similar to those achieved with the fresh catalyst. This is an advantage of heterogeneous catalysis over homogeneous systems, not to mention that solid catalysts overcome difficulties concerning catalyst solubility in homogeneous catalysis. These facts, added to the apparent failure to observe catalyst deactivation in heterogeneous systems, make catalyst immobilization an interesting alternative to homogeneous systems.

7. Conclusion

The obtained FePor-LDH-X solids displayed good catalytic properties under the investigated conditions. Preliminary results demonstrated that the materials were catalytically active in the oxidation of cyclooctene and cyclohexane by PhIO, as expected for immobilized FePor. Also, the immobilized FePor-LDH-TEA solid retained its catalytic activity during recycling procedures, not to mention that it was able to oxidize the terminal position of heptane, which is unusual when metalloporphyrins are used as catalyst. We can suppose that the influence of the support environment on substrate access to the active catalytic center is responsible for such regioselectivity, as well as the positioning of the catalyst in the support.

Acknowledgments

The authors are grateful to Conselho Nacional de Desenvolvimento Científico e Tecnológico (CNPq), Coordenação de Aperfeiçoamento de Pessoal de Nível Superior (CAPES), Fundação Araucária, Fundação da Universidade Federal do Paraná (FUNPAR), and Universidade Federal do Paraná (UFPR) for financial support.

References

[1] A.A. El-Awady, P.C. Wilkins, R.G. Wilkins, Inorg. Chem. 24 (1985) 2053–2057.
[2] D. Mansuy, Coord. Chem. Rev. 125 (1993) 129–142.
[3] F. Bedioui, Coord. Chem. Rev. 144 (1995) 39–68.
[4] J. Haber, L. Matachowski, K. Pamin, J. Poltowicz, J. Mol. Catal. A: Chem. 198 (2003) 215–221.
[5] J.T. Groves, J. Inorg. Biochem. 110 (2006) 434–447.
[6] D. Mansuy, C. R. Chim. 10 (2007) 1–22.
[7] F.L. Benedito, S. Nakagaki, A.A. Saczk, P.G. Peralta-Zamora, M.C.M. Costa, Appl. Catal. A Gen. 250 (2003) 1–11.
[8] Y. Iamamoto, Y.M. Idemori, S. Nakagaki, J. Mol. Catal. A: Chem. 99 (1985) 187–193.
[9] M.A. Matinez-Lorente, P. Battioni, W. Kleemiss, J.F. Bartoli, D. Mansuy, J. Mol. Catal. A: Chem. 113 (1996) 343–353.
[10] V. Rives, M.A. Ullibarri, Coord. Chem. Rev. 181 (1999) 61–120.
[11] J. Tronto, F. Leroux, E.L. Crepaldi, Z. Naal, S.I. Klein, J.B. Valim, J. Phys. Chem. Solids 67 (2006) 968–972.
[12] M. Halma, K.A.D.F. Castro, C. Taviot-Gueho, V. Prévot, C. Forano, F. Wypych, S. Nakagaki, J. Catal. 257 (2008) 233–243.
[13] L. Li, R. Ma, Y. Ebina, N. Iyi, T. Sasaki, Chem. Mater. 17 (2005) 4386–4391.
[14] R. Marangoni, C. Taviot-Guého, A. Illaik, F. Wypych, F. Leroux, J. Coll. Interf. Sci. 326 (2008) 366–373.
[15] F. Wypych, K.G. Satyanarayana, Clay Surfaces: Fundamentals and Applications, Elsevier, Amsterdam, 2004.
[16] V. Rives, Layered Double Hydroxides: Present and Future, Nova Science, New York, 2001.
[17] C.R. Gordijo, V.R.L. Constantino, D.O. Silva, J. Solid State Chem. 180 (2007) 1967–1976.
[18] V. Prevot, C. Forano, J.P. Besse, J. Solid State Chem. 153 (2000) 301–309.
[19] S. Aisawa, S. Sasaki, S. Takahashi, H. Hirahara, H. Nakayama, E. Narita, J. Phys. Chem. Solids 67 (2006) 920–925.
[20] V. Prevot, C. Forano, J.P. Besse, Appl. Clay Sci. 18 (2001) 3–15.
[21] S. Vial, V. Prevot, F. Leroux, C. Forano, Micropor. Mesopor. 107 (2008) 190–201.
[22] S. Nakagaki, M. Halma, A. Bail, G.G.C. Arízaga, F. Wypych, J. Coll. Interf. Sci. 281 (2005) 417–423.
[23] F. Wypych, G.G.C. Arízaga, Quim. Nova 28 (2005) 24–29.
[24] S. Bonnet, C. Forano, J. Besse, Mat. Res. Bull. 33 (1998) 783–788.
[25] S. Nakagaki, F. Wypych, J. Coll. Interf. Sci. 315 (2007) 142–157.
[26] S. Nakagaki, G.S. Machado, M. Halma, A.A.S. Marangon, K.A.D.F. Castro, N. Mattoso, F. Wypych, J. Catal. 242 (2006) 110–117.
[27] M. Halma, A. Bail, F. Wypych, S. Nakagaki, J. Mol. Catal. A: Chem. 243 (2006) 44–51.
[28] Y. Liu, E. Lotero, J.G. Goodwin Jr., X. Mo, Appl. Catal. A: Gen. 331 (2007) 138–148.
[29] E.L. Crepaldi, J.B. Valim, Quim. Nova 21 (3) (1998) 300–311.
[30] V.R.R. Cunha, A.M.C. Ferreira, V.R.L. Constantino, J. Tronto, J.B. Valim, Quim. Nova 33 (1) (2010) 159–171.
[31] S. Nakagaki, K.A.D.F. Castro, G.S. Machado, M. Halma, S.M. Drechsel, F. Wypych, J. Braz. Chem. Soc. 17 (2006) 1672–1678.
[32] J.G. Sharefkin, H. Saltzmann, Org. Synth. 43 (1963) 62–64.
[33] J. Lucas, E.R. Kennedy, M.W. Forno, Org. Synth. 43 (1963) 483–1483.
[34] J. Inacio, C. Taviot-Guého, C. Forano, J.P. Besse, Appl. Clay Sci. 18 (2001) 255–264.
[35] S. Letaief, C. Detellier, Chem. Commun. (2007) 2613–2615.
[36] N. Iyi, T. Sasaki, Appl. Clay Sci. 42 (2008) 246–251.
[37] L. Zhang, J. Zhu, X. Jiang, D.G. Evans, F. Li, J. Phys. Chem. Solids 67 (2006) 1678–1686.
[38] J.J. Moulaur, W.F. Stickle, P.E. Sobol, K.D. Bomben, Handbook of X-ray Photoelectron Spectroscopy, Phys. Eletron. Inc., Minnesota, 1995.
[39] A. Maciuca, E. Dumitriu, F. Fajula, V. Hulea, Appl. Catal. A: Gen. 338 (2008) 1–8.
[40] F. Li, Y. Wang, Q. Yang, D.G. Evans, C. Forano, X. Duan, J. Hazard. Mater. B 125 (2005) 89–95.
[41] K. Nakamoto, Infrared and Raman Spectra of Inorganic and Coordination Compounds, 5th ed., 1997.
[42] F. Leroux, J. Gachan, J.P. Besse, J. Solid State Chem. 177 (2004) 245–250.
[43] M. Halma, F. Wypych, S.M. Dreschel, S. Nakagaki, J. Porph. Phthal. 6 (2002) 502–513.
[44] F.S. Vinhado, P.R. Martins, A.P. Masson, D.G. Abreu, E.A. Vidoto, O.R. Nascimento, Y. Iamamoto, J. Mol. Catal. A: Chem. 188 (2002) 141–151.
[45] S.L.H. Rabelo, A.R. Gonçalves, M.M.Q. Simões, M.G.P. Neves, J.A.S. Cavaleiro, J. Mol. Catal. A: Chem. 256 (2006) 321–333.
[46] R.M. Hanson, Chem. Rev. 91 (1991) 437–475.
[47] D.R. Leanord, J.R. Lindsay-Smith, J. Chem. Soc. Perkin Trans. 2 (1991) 25–30.
[48] P. Inchley, J.R. Lindsay-Smith, R.J. Lower, New J. Chem. 13 (1989) 669–676.
[49] D. Dolphin, T.G. Traylor, L.Y. Xie, Acc. Chem. Res. 30 (1997) 251–259.
[50] J.T. Groves, R.C. Haushalter, M. Nakamura, T.E. Nemo, B.J. Evans, J. Am. Chem. Soc. 103 (1981) 2884–2886.
[51] J.T. Groves, T.E. Nemo, R.S. Meyers, J. Am. Chem. Soc. 101 (1979) 1032–1033.
[52] A.T. Papacídero, L.A. Rocha, B.L. Caetano, E. Molina, H.C. Sacco, E.J. Nassar, Y. Martinelli, C. Mello, S. Nakagaki, K.J. Ciuffi, Colloids Surf. A 275 (2006) 27–35.
[53] A.J. Appleton, S. Evans, J.R. Lindsay-Smith, J. Chem. Soc. Perkin Trans. 2 (1995) 281–285.
[54] S.A. El-Safty, Y. Kiyozumi, T. Hanaoka, F. Mizukami, Appl. Catal. A: Gen. 337 (2008) 121–129.
[55] S. Campestrini, F. Furia, P. Ghiotti, F. Novello, C. Travaglini, J. Mol. Catal. A: Chem. 105 (1996) 17–23.
[56] P.R. Cooke, J.R. Lindsay-Smith, J. Chem. Soc. Perkin. Trans. 1 (1994) 1913–1923.
[57] P. Battioni, J.P. Renaud, J.F. Bartoli, M. Reina-Artiles, M. Fort, D. Mansuy, J. Am. Chem. Soc. 110 (1988) 8462–8470.
[58] B.R. Cook, T.J. Reinert, K.S. Suslick, J. Am. Chem. Soc. 108 (1986) 7281–7286.
[59] J.M. Thomas, R. Raja, G. Sankar, R.G. Bell, Acc. Chem. Res. 34 (2001) 191–200.